ELSEVIER

Physica D 149 (2001) 107–122

PHYSICA D

www.elsevier.com/locate/physd

Parametric forcing of scroll-wave patterns in three-dimensional excitable media

Rolf-Martin Mantel [a], Dwight Barkley [b,*]

[a] *Department of Mathematics and Computer Science, Phillips University, Hans-Meerwein Strasse, D-35032 Marburg, Germany*
[b] *Mathematics Institute, University of Warwick, Coventry CV4 7AL, UK*

Received 13 October 1998; received in revised form 3 August 2000; accepted 11 September 2000
Communicated by C.K.R.T. Jones

Abstract

The dynamics of axisymmetric and twisted scroll rings under homogeneous periodic forcing is studied numerically. The collapse of axisymmetric rings can be enhanced or retarded significantly with resonant forcing. Twisted scroll rings exhibit the phenomenon of resonant drift in a direction normal to the axis of the central filament. The scaling of mean and fluctuating axial drift due to forcing is determined. Evidence is provided showing that the appropriate symmetry group for the dynamics of the unforced twisted scroll ring is $\mathbb{SE}(2) \times \mathbb{R}$. Ordinary differential equations based on symmetry considerations explain the dynamics without resorting to laws of filament motion and the local geometry hypothesis.

Keywords: Excitable media; Euclidean symmetry; Scroll wave; Parametric forcing

1. Introduction

Wave propagation in reaction–diffusion systems with excitable dynamics occurs in a wide variety of chemical and biological contexts. Examples include unstirred Belousov–Zhabotinsky reagent [1,2], catalytic surface reactions [3], *Xenopus* eggs [4], and cardiac tissue [5,6]. This last example is particularly important because waves of electrical activity are thought to be responsible for certain types of cardiac abnormalities (arrhythmias) leading to death [5–7]. In two-space dimensions, waves in excitable systems typically take the form of spirals rotating about a point that is roughly fixed in space [2], although complex dynamics (meandering) is also observed [8,9]. In three-space dimensions one finds scroll waves that are organized around one-dimensional curves known as filaments. The geometry of these filaments ranges in complexity from simple rings to complicated links, knots, and tangles [10–15].

In this paper we consider what happens to scroll waves when parametric forcing is applied homogeneously to a three-dimensional excitable medium. To motivate this study we first recall the basic phenomenology of homogeneous parametric forcing of spiral waves in a two-dimensional excitable medium. This problem has been considered extensively experimentally and theoretically [16–27]. Fig. 1 summarizes the most notable effect of weak forcing on a rotating spiral wave. In Fig. 1(a) is shown a rotating spiral wave in a standard reaction–diffusion model of excitable media (presented in the next section). The

* Corresponding author.
E-mail addresses: mantel@mathematik.uni-marburg.de (R.-M. Mantel), barkley@maths.warwick.ac.uk (D. Barkley).

0167-2789/01/$ – see front matter
PII: S0167-2789(00)00185-8

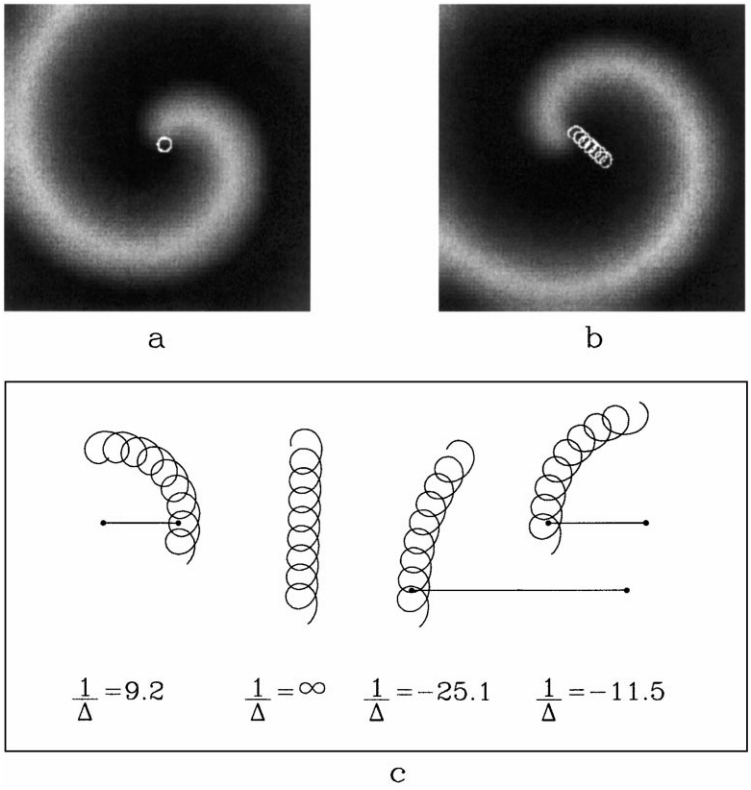

Fig. 1. Effects of periodic forcing on spiral-wave dynamics. (a) Periodically rotating solution of the reaction–diffusion model considered in this paper (model parameters are: $a = 0.8$, $b = 0.05$, and $\epsilon = 0.02$). Gray-scale shows values of the slow species and the white curve shows the path of the spiral tip. (b) Conditions as in (a), except with parametric forcing in 1–1 resonance with the spiral rotation frequency, $(b = 0.05 + 0.0035\sin(1.7434t))$. (c) The effect of parametric forcing in the vicinity of a 1–1 resonance. Δ denotes the frequency detuning and line segments show the secondary radius R_2 of the "tip paths".

spiral rotates about a fixed center with frequency ω_1 and the path of the tip is a circle. Fig. 1(b) shows that a linear drift can be produced by resonant parametric forcing of the medium: forcing frequency ω_f equal to the natural frequency ω_1. Fig. 1(c) shows the dynamics for forcing near such a resonance. Letting $\Delta = \omega_1 - \omega_f$ denote the detuning between natural and forcing frequency, and R_2 denote the large secondary radius resulting from the forcing, then in the vicinity of the resonance these are related by $R_2 \sim 1/\Delta$, and at resonance ($\Delta = 0$), $R_2 = \infty$. The drift speed at resonance grows as the amplitude of the forcing (not shown). Note that the curves in Fig. 1(c) are not from reaction–diffusion simulations but rather from ordinary differential equations based on the relevant symmetries of the system [26].

The primary motivation for our study is to understanding forced spatio-temporal patterns from the point of view of symmetric bifurcation theory. The two-dimensional case is well understood [26,27], but only recently has analysis been undertaken of periodic forcing on three-dimensional structures in excitable media using bifurcation theory [28]. This dynamical-systems approach to understanding spiral and scroll wave dynamics is important because it offers an alternative to the laws of filament dynamics most often used as a theoretical basis for understanding scroll-wave behavior [13,14,29–32].

A secondary motivation for considering periodic forcing comes from potential applications to cardiology. The spiral motion resulting from resonant or near resonant forcing on spiral waves, as illustrated

in Fig. 1, has been known for some time and this effect has been proposed as a method for treating certain cardiac arrhythmias [16–18,20,23,24]. The idea is to use periodic or nearly periodic voltage stimuli to remove spiral waves from cardiac tissue by inducing drift of an offending spiral wave to a boundary (e.g. the heart's surface) where the wave cannot be sustained. The potential advantage here is that treatment can be accomplished using considerably lower voltages than are currently required in cardiac defibrillators. Heart tissue is three-dimensional, however, and so it is of some interest to understand how parametric forcing acts in the case of three-space dimensions. A preliminary understanding the dynamics of these waves in the absence of the complexities of heart models is of fundamental importance. As far as we are aware, there have been no published numerical or experimental studies of how parametric forcing affects scroll waves.

We shall address what happens to scroll waves when weak, homogeneous parametric forcing is applied to a three-dimensional excitable medium and to what extent the resulting dynamics can be understood from low-dimensional dynamical-systems analysis. We consider briefly the axisymmetric scroll ring, but focus mainly on the twisted-scroll ring. We provide accurate numerical data for the dynamics and compare with predictions of dynamical-systems theory.

2. Model and methods

For our numerical simulations, we use the two-variable reaction–diffusion equations

$$\frac{\partial u}{\partial t} = f(u,v) + \nabla^2 u,$$
$$\frac{\partial v}{\partial t} = g(u,v) + D_v \nabla^2 v, \tag{1}$$

where the functions $f(u,v)$ and $g(u,v)$ express the local reaction kinetics of the two variables u and v. The diffusion coefficient for the u variable is scaled to unity, and thus D_v is the ratio of diffusion coefficients. For the reaction kinetics, we use

$$f(u,v) = \frac{1}{\varepsilon} u(1-u)(u - u_{\mathrm{th}}(v)),$$
$$g(u,v) = u - v \tag{2}$$

with $u_{\mathrm{th}}(v) = (v+b)/a$. This choice differs from traditional FitzHugh–Nagumo equations in a way that allows for fast computer simulations [33,34]. We apply periodic forcing by sinusoidally varying the excitability threshold through the parameter b: $b(t) = b_0 + A\cos(\omega_{\mathrm{f}} t)$. The amplitude A and frequency ω_{f} (or equivalently period $T_{\mathrm{f}} = 2\pi/\omega_{\mathrm{f}}$) of the forcing are the parameters varied in this study. We keep the other model parameters fixed at $a = 0.8$, $b_0 = 0.01$, $\varepsilon = 0.02$, and $D_v = 0$. Without forcing, the medium is strongly excitable. In two dimensions, the equations generate rigidly rotating spirals with small cores very similar to that shown in Fig. 1(a). These spirals are far from the meander instability [35] and initial conditions converge quickly to rotating waves.

We use a third-order semi-implicit scheme to time-step f, combined with explicit Euler time-stepping for g and the Laplacian term. In the evaluation of f and in the diffusion of u, we take into account that $u \simeq 0$ in a large part of the domain, and that $f(0,v) = 0$. We use a 19-point stencil with good numerical properties (isotropic error, mild time-step constraint) for approximating the Laplacian operator. Neumann boundary conditions are imposed in the horizontal (x and y) directions. We generally impose periodic boundary conditions in the z-direction to allow solutions to move freely in that direction, although we have carried out some tests with Neumann boundary conditions in the z-direction as explained in Section 3.2.1. We initially simulate with numerical parameters corresponding to moderate resolution: square box of length $L = 36$ on a side, grid spacing $h = \frac{3}{7}$, time-step $\Delta t/\epsilon = 2.4$. For high accuracy studies of the twisted scroll ring, we use a higher resolution of $L = 24$, $h = \frac{2}{7}$, $\Delta t/\epsilon = 0.6$. Complete numerical details for the three-dimensional simulations are given in [34].

We define the scroll filament to be the intersection of the two iso-surfaces $u = \frac{1}{2}$ and $v = u_{\mathrm{th}}(\frac{1}{2})$. In two dimensions this defines the spiral tip [33]. For parameter values in this study, two-dimensional spirals trace

out small circles (similar to that in Fig. 1). In three dimensions, filaments undergo small-scale circulations at the period of wave rotations (corresponding to rotations in two dimensions) and also slower large-scale motions associated with movement of the scroll structures in three-space. We are primarily interested in these slow motions.

Focusing on filaments rather than the full concentration fields reduces the complexity of the structures to be analyzed. However, even this is not sufficient to obtain a low-dimensional description of scroll waves. For the waves we consider here the filaments are or are close to simple geometric objects (lines and circles) and this allows us to reduce the infinite-dimensional dynamics to the dynamics of simple geometric objects described by a few coordinates (centers, radii, etc.) and we need only to save this small number of quantities during long simulations. For scroll rings, the obvious object to fit is a circle. For axisymmetric rings, the numerically computed filaments are circles to within numerical precision. For twisted rings, the filament is composed of two pieces, one approximately a line and the other approximately a circle. We focus on the nearly circular part of the filament and find the best approximating circle.

We have used the following algorithm for our fitting. First consider finding a best fit sphere to a set of points (x_i, y_i, z_i) in three dimensions [36]. Defining $Q_i = x_i^2 + y_i^2 + z_i^2$, the following set of equations gives the center (a, b, c) of the sphere:

$$a\begin{pmatrix}\mathrm{var}(x)\\ \mathrm{covar}(x,y)\\ \mathrm{covar}(x,z)\end{pmatrix} + b\begin{pmatrix}\mathrm{covar}(x,y)\\ \mathrm{var}(y)\\ \mathrm{covar}(y,z)\end{pmatrix} + c\begin{pmatrix}\mathrm{covar}(x,z)\\ \mathrm{covar}(y,z)\\ \mathrm{var}(z)\end{pmatrix} = \frac{1}{2}\begin{pmatrix}\mathrm{covar}(x,Q)\\ \mathrm{covar}(y,Q)\\ \mathrm{covar}(z,Q)\end{pmatrix}, \qquad (3)$$

where var and covar refer to variance and covariance of the data points. The radius then is calculated as

$$r = \sqrt{a^2 + b^2 + c^2 + \bar{Q} - 2a\bar{x} - 2b\bar{y} - 2c\bar{z}},$$

where $\bar{x} = \mathrm{mean}(x)$, etc. Eq. (3) becomes nearly singular if the points are nearly coplanar as in the case of a scroll ring. The size of the eigenvalue closest to zero gives a measure of how close the points are to a plane, and the associated normalized eigenvector gives a unit normal for a family of planes. Replacing the nearly singular direction with the equation of the plane going through the mean position $(\bar{x}, \bar{y}, \bar{z})$ allows us to calculate the center and radius of the best fit circle, which we denote (X, Y, Z) and R, respectively. In this way full concentration fields are projected onto four scalars. In addition, we output the unit normal vector and the error in the fit. The latter is used to assess the validity of fitting a circle to the approximately circular filament of the twisted scroll ring in Section 3.

3. Results

3.1. Axisymmetric scroll rings

A scroll ring is an axisymmetric solution of the reaction–diffusion equations which contains a spiral pattern in each azimuthal slice; see Fig. 2. The filament formed from the "tips" of these spirals is a planar ring. We take the axis of symmetry to be the z-axis. The dynamics of scroll rings are necessarily limited to changes in radius, R, and position, Z, along the axis of symmetry. In a singly diffusive medium ($D_v = 0$) it is well established that an axisymmetric ring drifts and shrinks at a speed inversely proportional to its radius (e.g. [13,15,37–39]).

Under parametric forcing of the medium, there are two possibilities for the behavior: either the solution becomes non-axisymmetric, in which case one could expect the scroll filament to become non-planar and possibly quite complicated, or else it remains axisymmetric, in which case the dynamics of the forced scroll ring can still be captured by measurements of R and Z. In practice we have limited ourselves to weak periodic forcing and have found no evidence of symmetry-breaking under these conditions.

For our numerical simulations, we start with an initial condition created by the complex polynomial $p(z_1, z_2) = z_2$ (see Appendix A). We then simulate for two to three rotations of the scroll in the absence of forcing to enable the scroll ring to settle into a state with approximately constant period. We take this state as an initial condition for our forcing experiments.

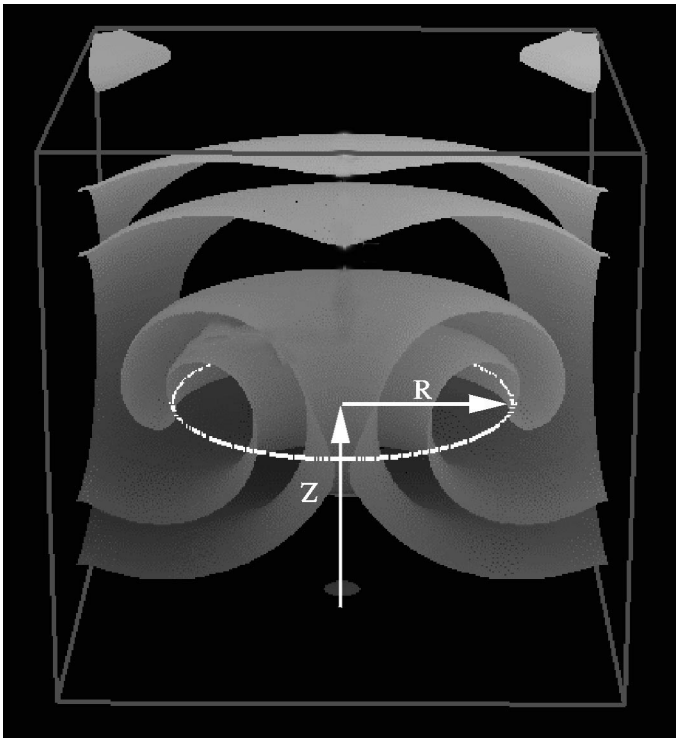

Fig. 2. Axisymmetric scroll ring. Shown is the iso-surface $u = \frac{1}{2}$ (clipped halfway through the volume). The filament (white) forms a planar ring parameterized by the radius R and location Z along the symmetry axis. Model parameters are as given in Section 2. The domain has sides of length $L = 40$.

The radius R and center (X, Y, Z) are obtained via the fitting procedure described in Section 2. The (X, Y) values of the center are found to be constant as expected for the axisymmetric ring. Note that while we simulate scroll rings in cubical domains, the solutions are axisymmetric to a high degree of precision. This is similar to the situation in two dimensions in which spiral waves behave as though in an infinite medium as long as the spiral centers are more than a wavelength from domain boundaries [35,40].

Fig. 3 shows filament paths for weak periodic forcing of a scroll ring in two cases, one near frequency resonance and the other away from resonance. Away from resonance, the scroll ring collapses in almost the same way as in the absence of forcing: the path in R–Z-coordinates is straight (averaged over the small-scale circular motions) until R becomes very small. The only difference between this and the unforced case is that the small-scale circular motions associated with the scroll wave rotations are slightly altered under forcing.

Close to resonance, however, there is a sizable deviation from straight line collapse in R–Z-coordinates. Recall the effect of parametric forcing on a spiral wave. As a frequency resonance is approached, the secondary radius of the quasiperiodic tip path grows as $R_2 \sim 1/\Delta$, where $\Delta \equiv \omega_1 - \omega_f$. Thus the near-resonant motion of the scroll ring can be understood simply as the large-scale quasiperiodic motion of a forced spiral wave (in R–Z-coordinates) superimposed on the natural shrink and drift dynamics. Note that the shrink and drift rates are themselves not constant but proportional to $1/R$. Thus as $R \to 0$, the shrink and drift speeds increase, whereas the bi-periodic motions due to forcing do not. This accounts for the uncoiling of the filament path as

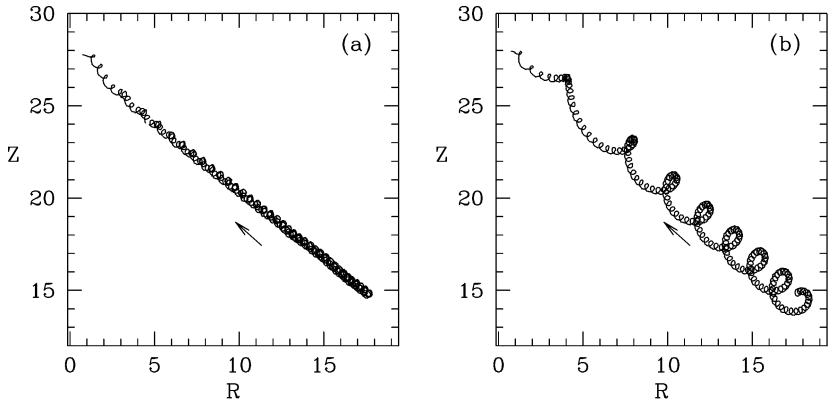

Fig. 3. Periodic forcing of a scroll ring. Plotted is the path of a scroll ring in R–Z-coordinates for (a) forcing away from resonance ($T_f = 4.2$) and (b) near resonant forcing ($T_f = 3.5$). The period of the unforced ring is not constant but $T_1 \approx 3.3$.

$R \to 0$. There is also a small shift in the rotation frequency of the scroll as $R \to 0$ but this seems to have little effect on the dynamics.

The fact that resonant forcing of a spiral wave induces a linear drift leads to the conjecture that resonant forcing at the appropriate amplitude and phase could be used to stabilize a collapsing scroll ring. That is, if the forcing-induced drift can be adjusted to counteract the shrink, then the radius of the scroll ring can be stabilized, though drift along the axis of symmetry would still occur. Likewise, for the same amplitude and frequency, but another choice of phase for the forcing it should be possible to greatly accelerate the ring collapse or to enhance the drift along the symmetry axis.

We have numerically tested this hypothesis and the results are shown in Fig. 4. Collapse of the scroll ring can be significantly accelerated or delayed with quite small forcing. With effort we have succeeded in stabilizing the scroll ring at a constant radius R for more than 100 wave rotations (over 300 time units). Thereafter the ring begins to collapse. Thus we have found that stabilization of the ring with fixed-frequency forcing is probably possible but difficult in practice because the resonance condition must be satisfied to a very high degree. The problem is compounded by the fact that once forcing is applied, the rotation frequency of the scroll changes slightly. It should be possible to completely stabilize a scroll ring either by further adjusting the forcing period and phase or by applying feedback control to the forcing.

In principle one could attempt a low-dimensional dynamical-systems description of the forced scroll ring (similar to the description considered in the following section of the twisted scroll ring). Ashwin and Melbourne [41] have done this by considering the scroll ring to be a stable state of the system. However, as axisymmetric scroll rings are nearly always transient structures we have not pursued a low-dimensional description of these states.

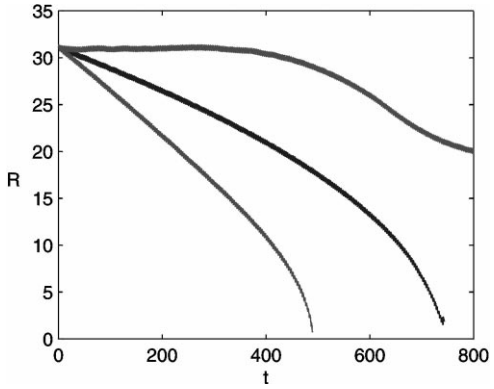

Fig. 4. Periodic forcing of a scroll ring. Plotted is R versus t for resonant periodic forcing ($T_f = 3.31$, $A = 0.00125$). Shown is no forcing (middle curve), forcing at a phase that gives most rapid collapse, and forcing at a phase that give maximum stabilization. Collapse of a scroll ring is delayed for approximately 100 wave rotations.

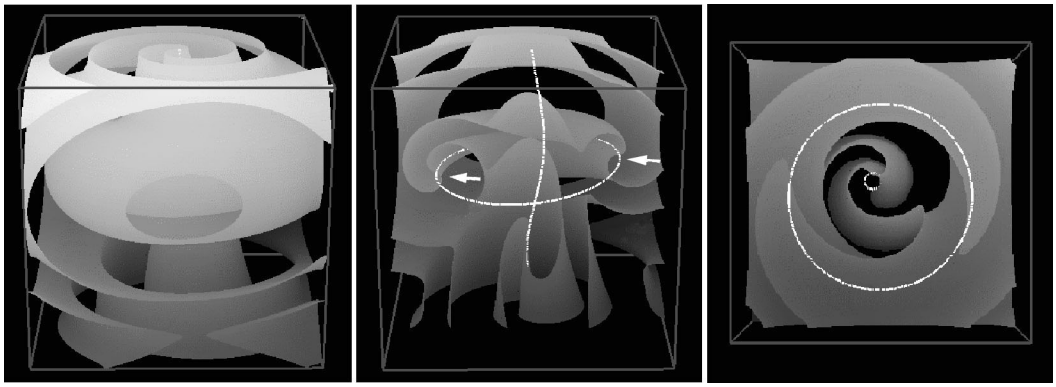

Fig. 5. Twisted scroll ring. Iso-surface $u = \frac{1}{2}$ (left), clipped iso-surface with filament (middle), and clipped iso-surface and filament from above (right). Arrows emphasize the change in "spiral phase" in rotating around the filament (cf. Fig. 2). Note, these images illustrate the structure of fields for the twisted ring, but this is not the asymptotic state. The domain has sides of length $L = 40$.

3.2. Twisted scroll rings

A twisted scroll ring is a solution to the reaction–diffusion equations with an approximately circular filament in which the phase of the "spiral" varies with azimuthal location. Instead the spiral phase changes around the ring by a multiple of 2π. We consider the simplest case of a once-twisted scroll ring (Fig. 5) for which the phase change is 2π. Topologically there must be another filament passing through the center of the filament ring [10], see also [13]. Thus even though one generally refers to the state as a twisted scroll ring, the filament consists of two pieces.

An initial condition for a twisted scroll ring is generated by the polynomial $p(z_1, z_2) = z_1 z_2$ (see Appendix A). The straight part of the filament is then parallel to the z-axis (the periodic direction in most of our simulations). Starting from the polynomial initial conditions, we simulate the reaction–diffusion equations long enough for the system to reach an asymptotic state. During the initial transient evolution, the ring shrinks until the interaction between the ring and the central filament stops the contraction. This final asymptotic state provides the initial condition used for our forcing experiments. The state in Fig. 5 is not this final asymptotic state, but we choose to show this early time state because the structure of the fields is clearly seen. Fig. 6 shows the filaments for the asymptotic state. It can be seen from the top view that the ring is indeed very close to circular and that the

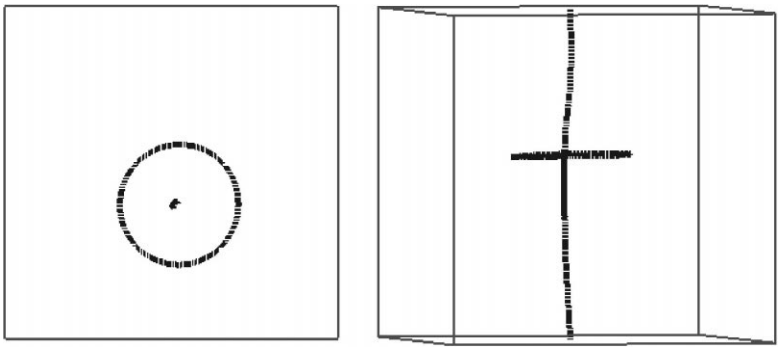

Fig. 6. Two views of the filament for the asymptotic twisted scroll ring. Top view showing projection onto x–y-coordinates (left) and side view with the z-axis vertical (right). The ring is nearly planar and the central filament is nearly straight and parallel to the z-axis. The domain has sides of length $L = 24$, that used for most simulations.

central filament is close to straight. Before describing the forcing studies, it is necessary to consider in some detail the dynamical properties of the unforced state.

3.2.1. Dynamics of the unforced twisted scroll ring

The important issue from our point of view is what symmetry group is appropriate for describing the dynamics of the state, for this will dictate a low-dimensional description of the forced dynamics. Unlike the untwisted scroll ring, the twisted scroll ring has no spatial symmetries (apart from the artificial periodic symmetry when periodic boundary conditions are imposed in our numerical treatment). This is why the ring is not exactly a circle in this case. However, the twisted scroll ring has a space–time symmetry: under time evolution the wave uniformly rotates and drifts according to

$$\mathbf{u}(t) = T_{c_1 t} R_{\omega_1 t} \mathbf{u}(0), \tag{4}$$

where $\mathbf{u} = (u, v)$, R_γ is a rotation through angle γ about some fixed axis, and T_d is a translation of distance d in that same direction. Hence ω_1 is the rotation frequency and c_1 is the drift speed. In our case the rotation axis is parallel to the z-axis so the drift is also in the z-direction.

To verify this, we have simulated the twisted ring for hundreds of wave rotations and have measured the drift and rotation of the solution. We then applied the inverse transformations to the time dependent solution: $T_{-c_1 t} R_{-\omega_1 t} \mathbf{u}(t)$. The resulting state was found to be steady, i.e. the twisted scroll ring is a *relative equilibrium* of the system. We have verified that to a high degree of precision the axis of rotation and direction of translation are parallel to the z-axis.

It is very significant that the rotation and translation axes align with the z-axis. It has been shown that in autonomous systems with three-dimensional Euclidean symmetry $\mathbb{E}(3)$, the evolution of a non-symmetric relative equilibria is generically rotation about an axis together with translation along the same axis [41–43]. This is as we have found. However, the symmetry analysis indicates that the axis points in an arbitrary direction. This is reasonable because a state with no spatial symmetry should drift in an arbitrary direction for there is nothing to determine a specific direction. However, this is not in agreement with our observation that the motion has a preferred direction: the z-axis.

It is possible that the imposed periodic boundary conditions in the z-direction are alone responsible for selecting this preferred direction and that in an infinite medium the axis of rotation and drift would not align with the central filament. We have conducted a number of numerical tests to examine the effect the imposed vertical boundary conditions have on this result. We have simulate twisted scroll rings in domains with large vertical extent, up to $L_z = 240$, with both periodic and Neumann boundary conditions to see if any evidence can be found for drift not aligned with the central filament.

The strongest numerical evidence that the vertical drift is not dictated by the vertical boundary conditions is the following; see Fig. 7. We have conducted simulations that can be run for a very long time without the need to impose periodic boundary conditions. We do this by imposing Neumann boundary conditions on all boundaries while effectively co-moving with the scroll ring. In these simulations, when the scroll ring drifts past the middle of the domain, the entire solution is moved downward exactly one grid spacing. Specifically, starting from the bottom of the domain, the solution on each horizontal grid plane is copied to the grid plane just below. The solution at the bottom plane of grid points (bottom boundary) is discarded and the solution at the top plane of grid points is unchanged. This is done every time the scroll ring crosses the middle of the domain. Hence the ring can be kept inside the domain during a long simulation without imposing periodic boundary conditions. At each step, the moving procedure affects only the solutions at the top-most and bottom-most grid planes. As a test of whether there are global consequences to this, we have considered different vertical domain lengths, up to $L_z = 120$ and find no variation in results with this length. We have also tested moving the solution downward by several grid points each time the scroll ring passes the midplane and find this has no measurable effect. We find in all simulations we have carried out that the asymptotic state of the system is

Fig. 7. Twisted scroll ring in a domain with Neumann boundary conditions on all sides. Upward drift of the scroll ring is compensated by appropriate downward motion of the fields (see text). $L_x = L_y = 24,\ L_z = 72$.

a relative equilibrium and that the drift is entirely in the vertical direction, i.e. parallel to the central filament.

We believe that even in an infinite medium the axis of rotation and drift would still align with the central filament. Our argument is as follows. Without loss of generality we can take the direction along which the central filament extends to infinity to be the z-direction. In each two-dimensional slice normal to the z-axis one finds a spiral pattern away from the axis. This can be seen to some extent in Fig. 5. As with usual two-dimensional spiral waves, these spirals behave nicely under rotations (around the z-axis) because small rotations result in small changes in the fields, even arbitrarily far from the axis. However, small rotations around any axis not parallel to the z-axis produce arbitrarily large changes in the fields, i.e. rotations act discontinuously on the state. Consider for example a small rotation around the x-axis. This would rotate the direction of the central filament and thus move the filament through a distance that would become unbounded as $z \to \infty$. Thus we argue that a twisted scroll ring in an infinite domain (supposing such a state exists) can be a relative equilibrium only if the axis of rotation and drift are aligned with the central filament.

We therefore conjecture that the relevant symmetries will include only the two-dimensional Euclidean symmetries in the plane perpendicular to the filament and the one-dimensional Euclidean symmetry along the axis of the central filament. Rotations about axes not parallel to the central filament should be excluded from a description of the dynamics. Thus the relevant symmetry group for the dynamics of a single twisted scroll ring is $\mathbb{SE}(2) \times \mathbb{R}$. This is consistent with our numerical experiments which are themselves representative both of other simulations and of what would occur experimentally.

3.2.2. Periodic forcing of a twisted scroll ring

We now turn to the effect of periodic forcing on the twisted scroll ring. In this section we present our numerical results and in Section 3.2.3 we discuss the interpretation in terms of dynamical-systems theory. Qualitatively, forcing does not change the wave fronts much away from the filament. Forcing can introduce significant changes in the shape of the filament, however (Fig. 8). The central filament is noticeably helical. The ring is distinctly oval, not centered around the central filament, and not confined to a plane. Despite this

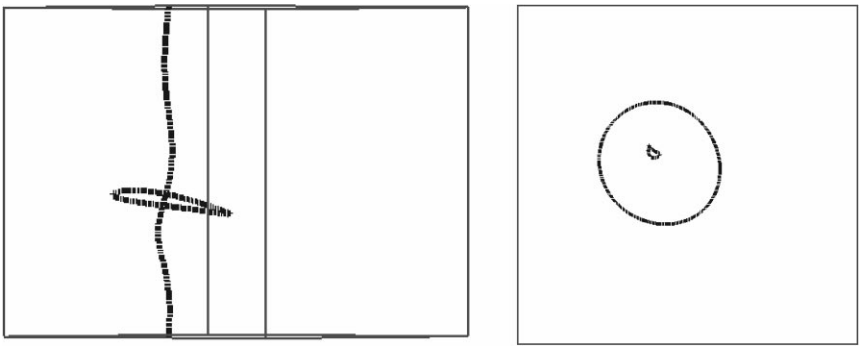

Fig. 8. Filaments of twisted scroll ring with parametric forcing. Forcing is at resonance $T_f = T_1 = 2.9925$ with amplitude $A = 0.002$. There is considerable change in shape from the unforced case.

the ring remains, in some sense, perpendicular to the filament where it passes through the ring's "center". While the ring is not circular, fitting to a circle is still a valid method for projecting onto a small number of variables: the "center" (X, Y, Z) and "radius" R.

The interesting dynamical aspects of the forced scroll ring along the filament axis (Z-coordinate) and perpendicular to the axis ((X, Y)-coordinates) are independent and thus we consider these separately. The important behavior in the X–Y dynamics is resonant drift. That is, if the twisted scroll ring is forced at resonance, then drift occurs in X–Y exactly as for spiral waves. This is shown in Fig. 9 where we plot X–Y paths for five forcing frequencies at fixed forcing amplitude. The similarity to the dynamics of spiral waves in Fig. 1 is apparent. (Note that in the absence of forcing, the dynamics in the X–Y plane is a rotating wave, i.e. the center of the best fit circle traces out a circular path.)

Typical drift dynamics in the Z-coordinate under periodic forcing is shown in Fig. 10. Not surprisingly, the instantaneous drift speed varies at the forcing period. What is at issue here is how the drift scales with forcing amplitude. To quantify this we define the instantaneous drift speed $c(t) = \mathrm{d}Z/\mathrm{d}t$, which can then be separated into mean and fluctuating parts $c(t) = c_1 + C(t)$, where $C(t)$ is periodic with zero mean over the forcing period: $\langle C(t)\rangle_{T_f} = 0$. In Fig. 11, we show the modification of the mean drift induced by forcing by plotting $c_1 - c_1^0$ as a function of forcing amplitude,

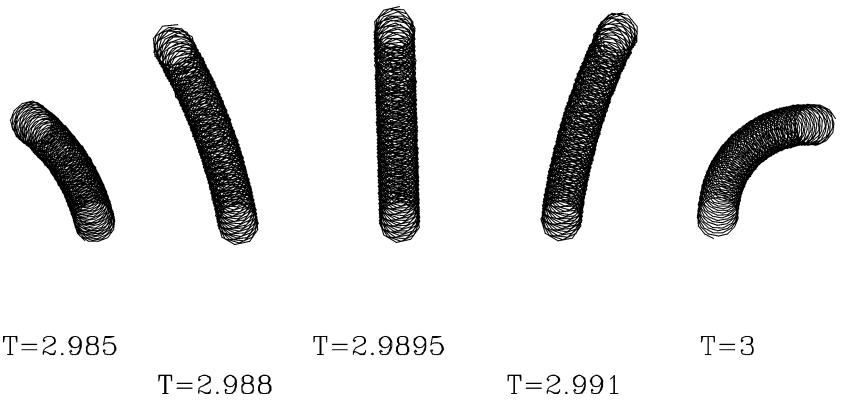

Fig. 9. The effect of near-resonant and resonant periodic forcing on the twisted scroll ring. The X–Y position of the "center" of the scroll ring is shown (see text). Five values of the forcing period T_f are shown at fixed forcing amplitude $A = 0.0005$.

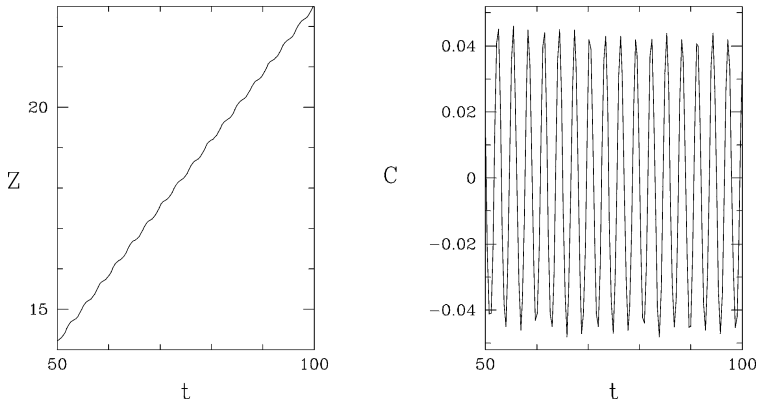

Fig. 10. Axial drift dynamics, $Z(t)$, under parametric forcing. Parameter values are $A = 0.001$ and $T_f = 2.9895$.

where c_1^0 is the drift without forcing. The mean drift speed is seen to scale as A^2 for small forcing amplitude. Fig. 12 shows $|C|$, the maximum of $C(t)$, as a function of forcing amplitude. Here it is seen that the magnitude of the fluctuating drift is proportional to forcing amplitude for small forcing. In summary, we find the following scalings as the forcing amplitude goes to zero: $c_1 - c_1^0 = \mathrm{O}(A^2)$ and $C(t) = \mathrm{O}(A)$.

3.2.3. Dynamical-systems description

One can understand qualitatively the dynamics of twisted scroll rings with simple ordinary differential equations (ODEs) incorporating appropriate symmetries. More specifically, the dynamics of these scrolls can be captured in terms of vector fields equivariant with respect to the correct symmetry group [28,42,43]. Assuming as discussed in Section 3.2.1 that the symmetry group for twisted scroll rings is $\mathbb{SE}(2) \times \mathbb{R}$, then the following ODEs can be obtained [28]:

$$\dot{\phi} = f_1(A, t), \qquad \dot{P} = \mathrm{e}^{\mathrm{i}\phi} f_2(A, t),$$
$$\dot{Z} = f_3(A, t), \tag{5}$$

where the variable $P = X + \mathrm{i}Y$ and the function f_2 are complex while ϕ, Z, f_1, and f_3 are real. A is the amplitude of forcing. Eqs. (5) are equivariant with

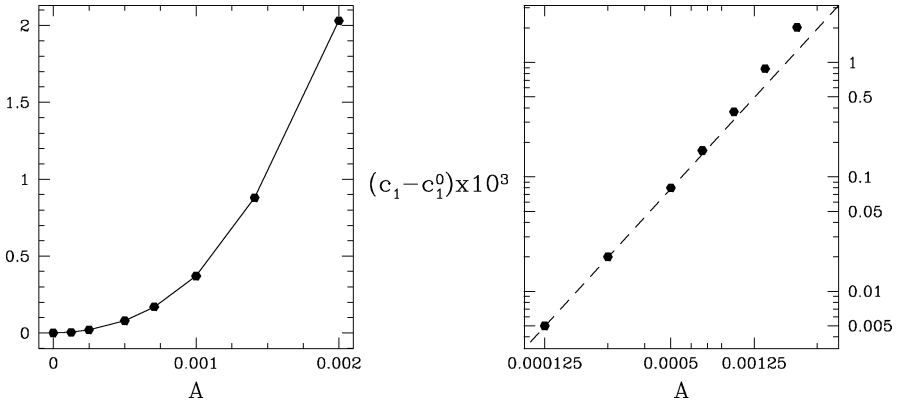

Fig. 11. Dependence of mean drift speed c_1 on forcing amplitude, where $c_1^0 = 0.165705$ is the drift speed without forcing. The dashed line has slope 2. The induced change is quadratic in the forcing amplitude.

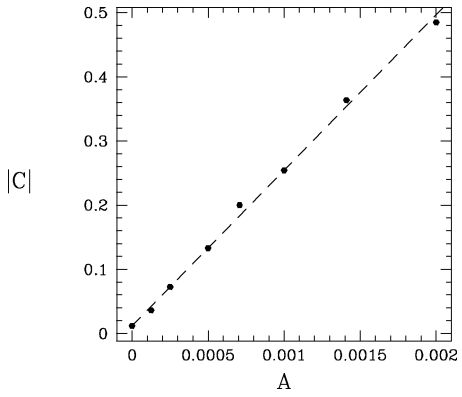

Fig. 12. Amplitude of the fluctuating drift as a function of forcing amplitude. Plotted is the maximum of the fluctuating drift $|C|$ normalized by the mean drift speed c_1. In the unforced case the drift speed varies by approximately $\pm 1\%$ due to numerical inaccuracies, while at a forcing amplitude of $A = 0.002$ the drift speed varies by nearly $\pm 50\%$.

respect to transformations of the group $\mathbb{SE}(2) \times \mathbb{R}$:

$$R_\gamma \begin{pmatrix} \phi \\ P \\ Z \end{pmatrix} = \begin{pmatrix} \phi + \gamma \\ \mathrm{e}^{\mathrm{i}\gamma} P \\ Z \end{pmatrix},$$

$$T_{abc} \begin{pmatrix} \phi \\ P \\ Z \end{pmatrix} = \begin{pmatrix} \phi \\ P + a + \mathrm{i}b \\ Z + c \end{pmatrix}, \tag{6}$$

where R_γ is rotation by angle γ about the vertical axis and T_{abc} is translation of (X, Y, Z) by (a, b, c). The triple (X, Y, Z) in the ODEs corresponds to a projection of twisted scroll solutions into $\mathbb{R}^3$. In particular, it corresponds to the position in physical space of essentially any well-defined, well-behaved point of the solution. We have in mind the center of the best fit circle used numerically to project the state of the system into $\mathbb{R}^3$, and hence we use the same notation in the ODE model (this should not cause any confusion).

In the absence of forcing ($A = 0$), the functions f_1, f_2, and f_3 are constants which we write as

$$f_1(0, t) = \omega_1, \qquad f_2(0, t) = s_1, \quad f_3(0, t) = c_1. \tag{7}$$

This corresponds to a state which rotates in X–Y-coordinates with frequency ω_1 and drifts in Z with speed c_1. To see this one integrates the $\dot{\phi}$-equation to obtain: $\phi(t) = \omega_1 t + \phi_0$. Substituting this into the equation for $\dot{P}$ gives:

$$\dot{P}(t) = s_1 \, \mathrm{e}^{\mathrm{i}(\omega_1 t + \phi_0)}. \tag{8}$$

Integrating this and the $\dot{Z}$-equation gives

$$P(t) = P_0 + R_1 \, \mathrm{e}^{\mathrm{i}(\omega_1 t + \phi_0 + \delta_1)}, \quad Z(t) = c_1 t + Z_0, \tag{9}$$

where $R_1 \equiv |s_1/\omega_1|$ and $\delta_1 = \mp\pi/2$ depending on the sign of s_1/ω_1.

Solution (9) then corresponds to a twisted scroll ring whose central filament is parallel to the z-axis. In the reaction–diffusion system there is a family of such states obtained by translations in three-space combined with rotations about the z-axis. In the ODE system this family is captured by the arbitrary constants P_0, ϕ_0, and Z_0. In our numerical simulations we impose Neumann boundary conditions in the x–y-directions and this means that the system is not exactly symmetric with respect to x–y translations and rotations about the vertical axis. However, in practice the effect of the boundaries is extremely weak as long as filaments do not get too close to the boundaries. This is exactly as for spiral waves and this is why the assumption of translational symmetry is appropriate for these waves [35,40].

If we consider all twisted scroll rings in the reaction–diffusion equations with filaments aligned with the vertical, then there are in fact four families of states related by two independent reflection symmetries not described by Eq. (5). One may reflect the system in z, or in the x–y plane, or both and thereby obtain other solutions. Reflecting in z gives a state that drifts in the opposite direction from the original, but rotates in the same direction. Reflecting in the x–y plane gives a state that drifts in the same direction but rotates in the opposite direction, and finally reflections in both directions give a state that drifts and rotates in the opposite direction from the original.

We now turn to the description of periodic forcing. For $A > 0$ the functions f_1, f_2, and f_3 are time-periodic with the forcing period $T_\mathrm{f} = 2\pi/\omega_\mathrm{f}$ [28]. The dynamics then follow almost exactly the treatment in [26–28]. In the ODE system the P, i.e.

X–Y, dynamics do not depend on the Z-dynamics and Eq. (5) for P is in fact as for two-dimensional rotating spiral waves. It is for this reason that the resonant drift dynamics of the scroll ring in Fig. 9 is identical to the resonant drift for spiral waves. The cause of the drift is essentially as follows. With periodic forcing at frequency ω_f, the equation for $\dot{P}$ will contain terms, in addition to those in (8), of the form

$$e^{i(\omega_1+k\omega_f)t}$$

for all integer k. Any term of this form integrates to a term of the same form as long as $\omega_1 + k\omega_f \neq 0$. At a resonance, where $\omega_1 + k\omega_f = 0$, integration gives a term in $P(t)$ that is linear in t: this is the resonant drift.

For the Z-dynamics, we must consider the form of f_3 for weak parametric forcing at frequency ω_f. Let the amplitude of the forcing be denoted ϵ and let c_1^0 be f_3 in the absence of forcing ($\epsilon = 0$). Then expanding in a Fourier series:

$$\begin{aligned} f_3(\epsilon, t) &= c_1^0 + \sum_{k=-\infty}^{\infty} \hat{c}_k(\epsilon)\, e^{ik\omega_f t} \\ &= [c_1^0 + \hat{c}_0(\epsilon)] + \left[\sum_{k\neq 0} \hat{c}_k(\epsilon)\, e^{ik\omega_f t}\right] \\ &= c_1 + \tilde{c}(t), \end{aligned} \tag{10}$$

where we have divided f_3 into its mean and fluctuating parts, c_1 and $\tilde{c}(t)$ respectively, both of which may depend on ϵ.

Integrating the $\dot{Z}$ equation, we have

$$Z(t) = c_1 t + C(t) + Z_0,$$

where

$$C(t) \equiv \int_0^t \tilde{c}(t')\, dt'.$$

For forcing with zero mean (as for the sinusoidal forcing applied to the reaction–diffusion equations) then $\hat{c}_0 = O(\epsilon^2)$ as shown by Wulff [44]. This gives the scalings found numerically in the reaction–diffusion simulations for the mean drift speed: $c_1 = c_1^0 + O(\epsilon^2)$.

For the fluctuating drift, one would expect that forcing at frequency ω_f would couple directly to the first Fourier mode in Eq. (10) to give a coefficient $\hat{c}_1$ scaling at first order in the forcing amplitude ϵ: $\hat{c}_1 = O(\epsilon)$. This agrees with the results from the reaction–diffusion simulations in which the fluctuating drift scales as $C = O(\epsilon)$ in the limit of small forcing.

4. Conclusion

We have accurately simulated two types of three-dimensional scroll structures in a reaction–diffusion model of excitable media with parametric forcing. Our particular focus has been on understanding the behavior of these states from a dynamical-systems viewpoint. For this we have projected the concentration fields of the reaction–diffusion equations into a four-dimensional space by computing scroll filaments and then fitting appropriate filaments to circles. We have shown that in principle it is possible to stabilize an axisymmetric scroll ring with parametric forcing. However, without some method of feedback control this is difficult in practice.

We verified that the unforced twisted scroll ring is a relative equilibrium of the reaction–diffusion equations (there is a frame of reference in which it is a steady state). We have argued on the basis of our numerical experiments that the dynamics of a twisted scroll ring are not those of a generic relative equilibrium in an $\mathbb{E}(3)$ equivariant system. Rather, the dynamics are governed by the symmetry $\mathbb{SE}(2) \times \mathbb{R}$. Finally we have carefully investigated twisted scroll rings under resonant and near-resonant periodic forcing and have shown that their behavior can be understood from the viewpoint of symmetric bifurcation theory, namely resonant drift occurs in a direction perpendicular to the central filament and drift along the central filament is modified.

The periodic forcing we have considered here is essentially equivalent to the dynamics near a Hopf bifurcation. The locus of Hopf bifurcations from rigid spiral rotation and to spiral meander in two dimensions is known [35] for the reaction–diffusion equations (1) and (2). It would be of some interest to consider the Hopf bifurcation undergone by the axisymmetric and

twisted scroll rings and in particular to establish where the instability occurs in parameter space.

Finally, we stress that the approach taken here to understanding waves in three-dimensional excitable media is very different from the approach of filament dynamics. The description of three-dimensional structures in terms of filament dynamics requires the "local geometry hypothesis" that filaments move according to their local curvature and twist which are generally assumed to be small [29–32]. These assumptions do not hold for most compact structures such as rings, links and knots, apparently because these structures exhibit substantial non-local filament interaction [13,14]. On the other hand, the dynamical-systems approach does not preclude filament interaction, but instead relies only on the basic symmetry properties of solutions. We hope to study other organizing centers (linked rings and knots) from this viewpoint in the future.

Acknowledgements

We wish to thank P. Ashwin, B. Fiedler, I. Melbourne, B. Sandstede, and especially C. Wulff for many valuable discussions. We also wish to acknowledge the hospitality of the Institute for Mathematics and its Applications, University of Minnesota, where portions of this work were carried out.

Appendix A

Here we describe the method used for generating initial conditions. This is essentially the method pioneered by Winfree et al.[1] which derives from a standard method of embedding an algebraic knot in three-space [47]. Think of a scroll wave as a stack of two-dimensional slices containing spirals. Then one can generate scroll initial conditions via two mappings: a mapping ϕ generating two-dimensional spirals with a known tip location, and a mapping f that stacks the spirals in the desired three-dimensional structure. The mapping ϕ is of the form $\phi : \mathbb{R}^2 \to \mathbb{R}^k$, where k is the number of fields. In our case $k = 2$, that is ϕ gives the two field values (u, v) at each point in the plane. The stacking map $f : \mathbb{R}^3 \to \mathbb{R}^2$ sends points in three-space to the two-dimensional slices. The composition $\phi \circ f$ thus assigns (u, v) values to each point in three-space, i.e. generates the initial conditions.

A.1. Two-dimensional spirals

A simple initial condition for spiral waves is a sector of excitation. Expressed in polar coordinates (r, θ), the excited region can be taken as lying between a wave front at $\theta = \theta_0$ and a wave back at $\theta = 0$. For kinetics (2), excited regions correspond to $u = 1$ and refractory regions to $u = 0$. Thus we take u to be initially piecewise constant with $u = 1$ for $0 \le \theta < \theta_0$, and $u = 0$ otherwise. We take v to be initially piecewise linear with $v = v_{\min} \simeq 0$ at the wave front and $v = v_{\max}$ at the wave back. Thus we have the following expression for ϕ:

$$\begin{pmatrix} r \\ \theta \end{pmatrix} \xrightarrow{\phi} \begin{cases} \begin{pmatrix} 1 \\ v_{\max} \dfrac{\theta_0 - \theta}{\theta_0} \end{pmatrix} & \text{if } \ 0 \le \theta < \theta_0, \\ \begin{pmatrix} 0 \\ v_{\max} \dfrac{\theta_0 - \theta}{\theta_0 - 2\pi} \end{pmatrix} & \text{if } \ \theta_0 \le \theta < 2\pi \end{cases} \tag{A.1}$$

where we have set $v_{\min} = 0$. In practice we use $v_{\max} = a$ and $\theta_0 \approx \pi$.

A.2. Complex polynomial maps

For simplicity assume that ϕ generates a spiral whose tip is at the origin in $\mathbb{R}^2$. (For the preceding ϕ this is approximately true.) Then the set of points in $\mathbb{R}^3$ that are mapped to the origin by the stacking map f comprise the filament. It is easy to find a continuous mapping that gives rise to a single straight scroll wave. However, as soon as filaments are joined to form rings, finding continuous maps with the appropriate kernel becomes more difficult.

[1] The method is due to D. Epstein, A. Winfree and T. Poston, unpublished in the original form (see [14,45,46]).

Interesting filaments geometries can be generated from complex polynomial maps. Given a non-constant polynomial in two complex variables $p(z_1, z_2)$, the equation $p(z_1, z_2) = 0$ describes a hyper-surface in $\mathbb{C}^2$. Denote this by V. Now look at the intersection of V with a small three-sphere $\mathbb{S}_\varepsilon$ centered about some point q on V and define $K = V \cap \mathbb{S}_\varepsilon$. As V is a two-dimensional manifold intersecting $\mathbb{S}_\varepsilon$ transversely, the real dimension of K must be one. In the simplest case K is a circle embedded into the three-sphere $\mathbb{S}_\varepsilon$. However, if q is a critical point of the polynomial, then K need not be topologically a circle, and if K is topologically a circle it can be embedded in a knotted way. This provides a method for obtaining the stacking map f itself as the composition of two mappings: $f = p \circ s$, where s maps $\mathbb{R}^3$ to a three-sphere in $\mathbb{R}^4$, and p is the polynomial mapping taking points in $\mathbb{C}^2 \cong \mathbb{R}^4$ to $\mathbb{C}$. The points in $\mathbb{R}^3$ that are mapped to the origin in $\mathbb{C}$ under the composition can be chosen via p to be some desired curve or curves.

The standard mapping from $\mathbb{R}^3$ into $\mathbb{S}^3_\varepsilon$ is the stereographic map:

$$\begin{pmatrix} x \\ y \\ z \end{pmatrix} \xrightarrow{s} \frac{1}{R^2+\varepsilon^2} \begin{pmatrix} 2\varepsilon^2 x \\ 2\varepsilon^2 y \\ 2\varepsilon^2 z \\ (R^2-\varepsilon^2)\varepsilon \end{pmatrix} \cong \frac{1}{R^2+\varepsilon^2} \begin{pmatrix} 2\varepsilon^2 x + \mathrm{i}2\varepsilon^2 y \\ 2\varepsilon^2 z + \mathrm{i}(R^2-\varepsilon^2)\varepsilon \end{pmatrix}, \quad \text{(A.2)}$$

where $R^2 \equiv x^2 + y^2 + z^2$. Points inside $\mathbb{S}^2_\varepsilon \subset \mathbb{R}^3$ are mapped to the lower hemisphere, points outside $\mathbb{S}^2_\varepsilon$ to the upper hemisphere of $\mathbb{S}^3_\varepsilon$.

In numerical simulations we are only interested in a subset of $\mathbb{R}^3$, usually a cube, and it is necessary to scale the simulation volume such that under the mapping (A.2) this volume covers a sizable portion of the sphere. Scaling the volume to the cube $[-2\varepsilon, 2\varepsilon]^3$ will cover over 70% of $\mathbb{S}^3_\varepsilon$, which is a good choice for most initial conditions. For the twisted scroll ring, it is necessary to scale the z-direction differently. Ideally the z-coordinate of the simulation cube should be scaled to $[-\infty, -\infty]$ and this can be accomplished via the tan function.

By appropriate choice of the polynomial map we can take $\varepsilon = \frac{1}{2}$ in the definition of s. Moreover, as we are only interested in a subset of $\mathbb{R}^3$, it is possible to use a simpler mapping by dropping the pre-factor in (A.2) and using

$$\begin{pmatrix} x \\ y \\ z \end{pmatrix} \xrightarrow{s} \begin{pmatrix} x \\ y \\ z \\ R^2 - \frac{1}{4} \end{pmatrix} \cong \begin{pmatrix} x + \mathrm{i}y \\ z + \mathrm{i}(R^2 - \frac{1}{4}) \end{pmatrix}. \quad \text{(A.3)}$$

This describes a parabolic surface that touches the sphere $\mathbb{S}^3_{1/4}$ at $(0, 0, 0, -\frac{1}{4})$.

In summary, we generate our initial conditions by scaling the simulation volume to the cube $[-1, 1]^3$, or $[-1, 1]^2 \times (-\infty, -\infty)$ for the twisted scroll ring, and then apply the following composition of mappings:

$$\underbrace{\mathbb{R}^3 \xrightarrow{s} \mathbb{C}^2 \xrightarrow{p} \mathbb{C}}_{f = p \circ s} \xrightarrow{\phi} \mathbb{R}^k.$$

where s is given by (A.3), p is chosen according to the desired filament structure, and ϕ is given by (A.1).

References

[1] A.N. Zaikin, A.M. Zhabotinsky, Nature 225 (1970) 535.

[2] A.T. Winfree, Spiral waves of chemical activity, Science 175 (1972) 634–636.

[3] S. Nettesheim, A. von Oertzen, H. Rotermund, G. Ertl, Reaction–diffusion patterns in the catalytic CO-oxidation on Pt(1 1 0) — front propagation and spiral waves, J. Chem. Phys. 98 (12) (1993) 9977–9985.

[4] J. Lechleiter, S. Girard, E. Peralta, D. Clapham, Spiral calcium wave-propagation and annihilation in xenopus-laevis oocytes, Science 252 (1991) 123–126.

[5] J.M. Davidenko, A.V. Pertsov, R. Salomonsz, W. Baxter, J. Jalife, Stationary and drifting spiral waves of excitation in isolated cardiac-muscle, Nature 355 (6358) (1992) 349–351.

[6] F.X. Witkowski, et al., Spatiotemporal evolution of ventricular fibrillation, Nature 392 (1998) 78–82.

[7] A.T. Winfree, Focus issue: fibrillation in normal ventricular myocardium, Chaos 8 (1998).

[8] W. Jahnke, W.E. Skaggs, A.T. Winfree, Chemical vortex dynamics in the Belousov–Zhabotinsky reaction and in the 2-variable oregonator model, J. Phys. Chem. 93 (1989) 740–749.

[9] G.S. Skinner, H.L. Swinney, Periodic to quasi-periodic transition of chemical spiral rotation, Physica D 48 (1991) 1–16.
[10] A.T. Winfree, S.H. Strogatz, Singular filaments organize chemical waves in 3 dimensions. 2. Twisted waves, Physica D 9 (1/2) (1983) 65–80.
[11] A.T. Winfree, S.H. Strogatz, Singular filaments organize chemical waves in 3 dimensions. 3. Knotted waves, Physica D 9 (3) (1983) 333–345.
[12] A.T. Winfree, S.H. Strogatz, Singular filaments organize chemical waves in 3 dimensions. 4. Wave taxonomy, Physica D 13 (1/2) (1984) 221–233.
[13] A.T. Winfree, Stable particle-like solutions to the nonlinear-wave equations of 3-dimensional excitable media, Siam Rev. 32 (1) (1990) 1–53.
[14] A.T. Winfree, Persistent tangles of vortex rings in excitable media, Physica D 84 (1/2) (1995) 126–147.
[15] A.T. Winfree, Lingering mysteries about organizing centers in the Beluzov–Zhabotinsky medium and its oregonator model, in: R. Kapral, K. Showalter (Eds.), Chemical Waves and Patterns, Kluwer Academic Publishers, Dordrecht, 1995, pp. 3–56.
[16] K.I. Agladze, V.A. Davydov, A.S. Mikhailov, Observation of a helical-wave resonance in an excitable distributed medium, JETP Lett. 45 (12) (1987) 767–770.
[17] V.A. Davydov, V.S. Zykov, A.S. Mikhailov, Kinematics of autowave patterns in excitable media, Uspekhi Fizicheskikh Nauk 161 (8) (1991) 45–86 (English Trans.; Sov. Phys. Usp. 34, 665).
[18] V.N. Biktashev, A.V. Holden, Resonant drift of an autowave vortex in a bounded medium, Phys. Lett. A 181 (3) (1993) 216–224.
[19] O. Steinbock, V. Zykov, S.C. Müller, Control of spiral-wave dynamics in active media by periodic modulation of excitability, Nature 366 (6453) (1993) 322–324.
[20] V.N. Biktashev, A.V. Holden, Design principles of a low-voltage cardiac defibrillator based on the effect of feedback resonant drift, J. Theoret. Biol. 169 (2) (1994) 101–112.
[21] M. Braune, A. Schrader, H. Engel, Entrainment and resonance of spiral waves in active media with periodically modulated excitability, Chem. Phys. Lett. 222 (4) (1994) 358–362.
[22] V. Zykov, O. Steinbock, S.C. Müller, External forcing of spiral waves, Chaos 4 (3) (1994) 509–518.
[23] V.N. Biktashev, A.V. Holden, Resonant drift of autowave vortices in 2 dimensions and the effects of boundaries and inhomogeneities, Chaos Solitons & Fractals 5 (3/4) (1995) 575–622.
[24] V.N. Biktashev, A.V. Holden, Control of reentrant activity in a model of mammalian atrial tissue, in: Proceedings of the Royal Society of London Series B — Biological Sciences, Vol. 260, No. 1358, 1995, pp. 211–217.
[25] A. Schrader, M. Braune, H. Engel, Dynamics of spiral waves in excitable media subjected to external periodic forcing, Phys. Rev. E 52 (1 PtA) (1995) 98–108.
[26] R.M. Mantel, D. Barkley, Periodic forcing of spiral waves in excitable media, Phys. Rev. E 54 (1996) 4791–4802.
[27] C. Wulff, Theory of meandering and drifting spiral waves in reaction–diffusion systems, Ph.D. Thesis, Freie Universität, Berlin, 1996.
[28] B. Sandstede, A. Scheel, C. Wulff, Bifurcations and dynamics of spiral waves, J. Nonlinear Sci. 9 (1999) 439–478.
[29] A.V. Panfilov, A.N. Rudenko, A.M. Pertsov, Twisted scroll waves in active 3-dimensional media, Dokl. Akad. Nauk SSSR 279 (4) (1984) 1000–1002.
[30] J.P. Keener, The dynamics of 3-dimensional scroll waves in excitable media, Physica D 31 (2) (1988) 269–276.
[31] V.N. Biktashev, Diffusion of autowaves — evolution equation for slowly varying autowaves, Physica D 40 (1) (1989) 83–90.
[32] V.N. Biktashev, A.V. Holden, H. Zhang, Tension of organizing filaments of scroll waves, Phil. Trans. Roy. Soc. London A 347 (1685) (1994) 611–630.
[33] D. Barkley, A model for fast computer-simulation of waves in excitable media, Physica D 49 (1/2) (1991) 61–70.
[34] M. Dowle, R.M. Mantel, D. Barkley, Fast simulations of waves in three-dimensional excitable media, Int. J. Bifur. Chaos 7 (11) (1997) 2529–2546.
[35] D. Barkley, Euclidean symmetry and the dynamics of rotating spiral waves, Phys. Rev. Lett. 72 (1) (1994) 164–167.
[36] M.J. Cohen, Fitting a circle to data points, newsgroup: sci.math, August 1996.
[37] A.V. Panfilov, A.M. Pertsov, Vortex ring in 3-dimensional active medium described by reaction–diffusion equations, Dokl. Akad. Nauk SSSR 274 (6) (1984) 1500–1503.
[38] W. Jahnke, C. Henze, A.T. Winfree, Chemical vortex dynamics in 3-dimensional excitable media, Nature 336 (6200) (1988) 662–665.
[39] A.V. Panfilov, A.N. Rudenko, V.I. Krinsky, Turbulent rings in 3-dimensional active media with diffusion by 2 components, Biofizika 31 (5) (1986) 850–854.
[40] D. Barkley, Spiral meandering, in: R. Kapral, K. Showalter (Eds.), Chemical Waves and Patterns, Kluwer Academic Publishers, Dordrecht, 1995, pp. 163–190.
[41] P. Ashwin, I. Melbourne, Noncompact drift for relative equilibria and relative periodic orbits, Nonlinearity 10 (1997) 595–610.
[42] B. Fiedler, B. Sandstede, A. Scheel, C. Wulff, Bifurcation from relative equilibria of noncompact group actions: skew products, meanders, and drifts, Documenta Mathematica 1 (1996) 479–505.
[43] B. Sandstede, A. Scheel, C. Wulff, Dynamics of spiral waves on unbounded domains using center-manifold reductions, J. Differential Equations 141 (1997) 122–149.
[44] C. Wulff, Transition from relative equilibria to relative periodic orbits, Doc. Math. J. DMV 5 (2000) 227–274.
[45] A.T. Winfree, When Time Breaks Down, Princeton University Press, Princeton, NJ, 1987.
[46] C. Henze, A.T. Winfree, A stable knotted singularity in an excitable medium, Int. J. Bifur. Chaos 1 (4) (1991) 891–922.
[47] K. Brauner, Zur Geometrie der Funktionen zweier komplexer Veränderlicher iii, iv, Abh. Math. Sem. Hamburg 6 (1928) 8–54.